Polymer Chemistry

Accepted Manuscript

ROYAL SOCIETY OF CHEMISTRY

www.rsc.org/polymers

Journal Name

ARTICLE

Macro-RAFT agent mediated dispersion copolymerization: a small amount of solvophilic co-monomer leads to a great change

Received 00th January 20xx,
Accepted 00th January 20xx

DOI: 10.1039/x0xx00000x

www.rsc.org/

Pengfei Shi, Heng Zhou, Chengqiang Gao, Shuang Wang, Pingchuan Sun* and Wangqing Zhang*

The macro-RAFT agent mediated dispersion copolymerization of two monomers, in which one is hydrophobic and the other is hydrophilic, is proposed to conveniently tune the morphology of the *in situ* synthesized block copolymer nano-objects. The poly(ethylene glycol) trithiocarbonate macro-RAFT agent mediated dispersion copolymerization of styrene and 4-vinylpyridine (St/4VP) in alcoholic solvent affords the *in situ* synthesis of the diblock copolymer nano-objects of poly(ethylene glycol)-*block*-poly(4-vinylpyridine-*co*-styrene) [PEG-*b*-P(4VP-*co*-St)]. It is found that, the morphology of the PEG-*b*-P(4VP-*co*-St) diblock copolymer nano-objects can be easily tuned either by changing the polymerization degree of the random P(4VP-*co*-St) block or the molar ratio of the PS/P4VP segments in the random P(4VP-*co*-St) block. The poly(ethylene glycol) trithiocarbonate macro-RAFT agent mediated dispersion copolymerization of St/4VP is compared with the dispersion RAFT polymerization of St, and the advantage of the dispersion RAFT copolymerization in tuning the block copolymer morphology is demonstrated. Our study is believed to a promising extension of the polymerization induced self-assembly (PISA) under dispersion RAFT polymerization.

1 Introduction

Block copolymer nano-objects have received much attention because of their potential applications for drug delivery, cosmetic, catalysis, stabilization of emulsions and surface coatings.[1-3] The popular strategy to prepare block copolymer nano-objects is through the micellization of amphiphilic block copolymer in the block selective solvent.[4-26] Following this strategy, a suitable pre-synthesized amphiphilic block copolymer is initially dissolved in a common solvent, then a block selective solvent is added to trigger the micellization of amphiphilic block copolymer, and finally the removal of the common solvent usually by dialysis is performed to afford block copolymer nano-objects frozen in the block selective solvent. Recently, we and others have demonstrated that the polymerization-induced self-assembly (PISA) offers a potentially decisive option for the *in situ* synthesis of block copolymer nano-objects through the macro-RAFT agent mediated polymerization under emulsion or dispersion condition.[27-50] Compared with the self-assembly of the pre-synthesized block copolymers in the block-selective solvent, the PISA strategy has two advantages. First, the preparation of the block copolymer nano-objects is achieved just simultaneously at the RAFT synthesis of the block copolymer, and therefore no additional procedures such as the dissolution of the block copolymer in a common solvent and the micellization triggering usually by adding a block-selective solvent are needed. Second, the PISA strategy affords the *in situ* synthesis of concentrated block copolymer nano-objects with the block copolymer concentration as high as 30 wt%, which is much beyond that in the micellization strategy. Up to now, following this PISA strategy especially at the case of macro-RAFT agent mediated dispersion polymerization, block copolymer nano-objects with various morphologies such as spheres, worms or rods and vesicles have been efficiently generated in non-aqueous or aqueous dispersion during the RAFT synthesis of amphiphilic block copolymers.[27-50]

In the *in situ* synthesis of block copolymer nano-objects through the macro-RAFT agent mediated dispersion polymerization, several parameters are found to dictate the size and morphology of the block copolymer nano-objects: (1) the composition of the block copolymer, *e.g.* the polymerization degree (DP) of the solvophilic block to the solvophobic blocks,[35-40] and the fraction of the solvophilic block and the solvophobic block in the block copolymers.[35,49,50] It is found that the short macro-RAFT agent mediated dispersion RAFT polymerization favorably leads to block copolymer worms or vesicles.[35,50] Besides, the DP of the solvophobic block is also firmly correlative to the size and/or morphology of the *in situ* synthesized block copolymer nano-objects.[38-50] With the DP of the solvophobic block increasing during the RAFT dispersion polymerization, the size of the block copolymer nano-objects increases or the morphology of the block copolymer nano-objects undergoes the transition from spheres to worms and lastly to vesicles;[35,39-44,49] and (2) the solvent character such as the solvent polarity and the monomer concentration.[35,36,39-

Key Laboratory of Functional Polymer Materials of the Ministry of Education, Collaborative Innovation Center of Chemical Science and Engineering (Tianjin), Institute of Polymer Chemistry, Nankai University, Tianjin 300071, China.
**To whom correspondence should be addressed. E-mail: spclbh@nankai.edu.cn; wqzhang@nankai.edu.cn.*
Electronic Supplementary Information (ESI) available: Fig. S1 showing ^{1}H NMR spectra of the polymerization solution and the equations, Table S1 summarizing the synthesized polymers, and Fig.S2-S4 showing the polymerization kinetics of the dispersion RAFT polymerization of St. See DOI: 10.1039/x0xx00000x

[42,49,50] By tuning the aforementioned parameters, block copolymer nano-objects with a predetermined morphology can be prepared.

In this contribution, the macro-RAFT agent mediated dispersion copolymerization of two monomers, in which one is hydrophobic and the other is hydrophilic, is proposed to tune the morphology of the *in situ* synthesized block copolymer nano-objects. The application of both a hydrophobic monomer and a hydrophilic monomer in dispersion RAFT copolymerization affords great convenience in tuning the hydrophobic/hydrophilic character of the block copolymer and therefore the morphology of the *in situ* synthesized block copolymer nano-objects. It is found that, in the RAFT dispersion copolymerization of styrene and 4-vinylpyridine mediated with the macro-RAFT agent of *S*-1-dodecyl-*S*′-(α,α′-dimethyl-α″-acetic acid) trithiocarbonate-terminated poly(ethylene glycol) monomethyl ether (PEG-TTC, in which TTC represents the RAFT terminal of trithiocarbonate), the morphology of the *in situ* synthesized block copolymer nano-objects of poly(ethylene glycol)-*block*-poly(4-vinylpyridine-*co*-styrene) [PEG-*b*-P(4VP-*co*-St)] can be conveniently tuned by changing the ratio of the fed hydrophobic/hydrophilic monomers of styrene/4-vinylpyridine (St/4VP). Comparison between the PEG-TTC macro-RAFT agent mediated dispersion polymerization of the single hydrophobic monomer of styrene to afford the poly(ethylene glycol)-*block*-polystyrene (PEG-*b*-PS) nano-objects and the PEG-TTC macro-RAFT agent mediated dispersion copolymerization of the St/4VP mixture is made, the advantage of conveniently tuning the block copolymer morphology in the dispersion RAFT copolymerization is demonstrated.

2 Experimental

2.1 Materials

The monomers of 4-vinylpyridine (4VP, 96%, Alfa) and styrene (St, >98%, Tianjin Chemical Company) were distilled under reduced pressure prior to use. Poly(ethylene glycol) monomethyl ether (PEG_{45}-OH, M_n = 2000 g/mol, Aldrich) was purified by azeotropic distillation with dry toluene before use. *S*-1-Dodecyl-*S*′-(α,α′-dimethyl-α″-acetic acid) trithiocarbonate (DDMAT) was synthesized as discussed elsewhere.[51] The initiator of 2,2′-azobis(2-methylpropionitrile) (AIBN, >99%, Tianjin Chemical Company) was purified by recrystallization from ethanol. Oxalyl chloride [$(COCl)_2$, 98%, Tianjin Chemical Company, China] was freshly distilled before use. Dichloromethane (DCM, >99%, Tianjin Chemical Company, China) was freshly distilled from CaH_2 prior to use. All the other chemical reagents were analytic grade and used as received. Deionized water was used in the present study.

2.2 Synthesis of poly(ethylene glycol) trithiocarbonate

The macro-RAFT agent of poly(ethylene glycol) trithiocarbonate (PEG_{45}-TTC, in which TTC represents the RAFT terminal of trithiocarbonate) was prepared by the esterification reaction of the hydroxy terminal in PEG_{45}-OH with the carboxyl group in DDMAT as described elsewhere.[52,53] Into a dry 100 mL flask, DDMAT (1.46 g, 4.00 mmol) and DCM (20.0 mL) were added, and subsequently dripping addition of oxalyl chloride [$(COCl)_2$, 1.7 mL, 20.0 mmol] dissolved in DCM (10.0 mL) in 10 min under nitrogen atmosphere was followed. The mixture was magnetically stirred under nitrogen atmosphere at 25 ^{0}C for about 2 h until the gas evolution stopped. The solvent and the excess oxalyl chloride were removed by rotary evaporation. Into the flask, PEG_{45}-OH (4.00 g, 2.00 mmol) dissolved in DCM (20.0 mL) was added, and the reaction was allowed to proceed for 24 h at 25 ^{0}C with magnetically stirring under nitrogen atmosphere. The solution was concentrated under reduced pressure, and the polymer was precipitated in *n*-hexane and dried in a vacuum oven at room temperature to afford the desired macro-RAFT agent of PEG_{45}-TTC (4.6 g, 96% yield).

2.3 PEG_{45}-TTC mediated dispersion (co)polymerization

The PEG_{45}-TTC macro-RAFT agent mediated RAFT dispersion copolymerization of St/4VP in the methanol/water mixture (80/20 by weight) was performed at 70 ^{o}C under $[St+4VP]_0$:$[PEG_{45}\text{-}TTC]_0$:$[AIBN]_0$ = 300~1200:3:1 and with the weight percent of the fed monomers plus the PEG_{45}-TTC macro-RAFT agent at 20 w%. Herein, a typical RAFT dispersion copolymerization under $[St]_0$:$[4VP]_0$:$[PEG_{45}\text{-}TTC]_0$:$[AIBN]_0$ = 900:300:3:1 is introduced. Into a 25 mL Schlenk flask with a magnetic bar, PEG_{45}-TTC (0.0452 g, 0.0192 mmol), St (0.6000 g, 5.76 mmol), 4VP (0.2019 g, 1.92 mmol), and AIBN (1.051 mg, 0.0064 mmol) dissolved in the 80/20 methanol/water mixture (3.3811 g) were added. The flask content was vigorously stirred, degassed with nitrogen, and then the polymerization was initiated by immersing the flask into preheated oil bath at 70 ^{o}C. After a given time, the polymerization was quenched by immersing the flask in iced water. To detect the monomers conversion, a drop of the polymerization solution (about 0.1 mL) was diluted with $CDCl_3$ (0.5 mL) and subjected to ^{1}H NMR analysis. The 4VP and St monomer conversion was calculated by following equations S1 and S2 (seeing the typical ^{1}H NMR spectra in Figure S1). To check the resultant block copolymer nano-objects, a small drop of the block copolymer colloidal dispersion was deposited onto a piece of copper grid, dried at room temperature under vacuum, and then observed by transmission electron microscope (TEM). To collect the polymer for the GPC and ^{1}H NMR analysis, the colloidal dispersion was precipitated into the mixture of diethyl ether and n-hexane (3:1 w/w), collected by three precipitation/filtration cycles, and then dried under vacuum at room temperature to afford the pale yellow block copolymer.

The referee experiment of the PEG_{45}-TTC macro-RAFT agent mediated RAFT dispersion polymerization of St was performed under the same conditions as those in the dispersion copolymerization introduced above.

2.4 Characterization

The ^{1}H NMR analysis was performed on a Bruker Avance III 400 MHz NMR spectrometer using $CDCl_3$ as solvent. The molecular weight and its distribution or the polydispersity index (PDI, PDI = M_w/M_n) of the synthesized polymers were determined by gel permeation chromatography (GPC) equipped with a Waters 600E GPC system, where THF was used as eluent and the narrow-polydispersity polystyrene was used as calibration standard. Transmission electron microscopy (TEM) observation was performed using a Tecnai G^2 F20 electron microscope at an acceleration of 200 kV.

3 Results and discussion

3.1 Synthesis of PEG_{45}-TTC

The poly(ethylene glycol) based macro-RAFT agent of PEG_{45}-TTC was prepared by the esterification reaction of the hydroxy terminal in the monohydroxyl terminated poly(ethylene glycol) with the carboxyl group in the trithiocarbonate of DDMAT as shown in Scheme 1A.[52] Following this method, DDMAT was first reacted with $(COCl)_2$ to afford the acyl chloride modified DDMAT, and then the esterification reaction between the acyl chloride modified DDMAT and the hydroxyl-terminated poly(ethylene glycol) was performed. To ensure complete esterification of the hydroxyl-terminated poly(ethylene glycol), 2-fold excess of the acyl chloride modified DDMAT was used. After esterification, the excess acyl chloride modified DDMAT was removed by depositing the macro-RAFT agent of PEG_{45}-TTC in n-hexane, in which the acyl chloride modified DDMAT is soluble and the poly(ethylene glycol) based macro-RAFT agent is insoluble, and therefore PEG_{45}-TTC was obtained.

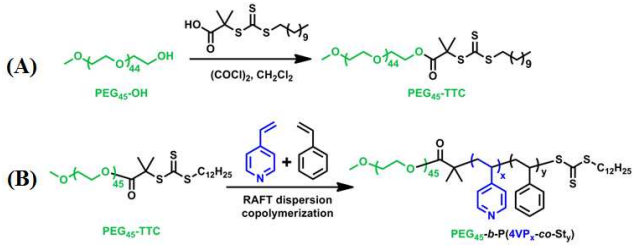

Scheme 1. Synthesis of PEG_{45}-TTC (A) and PEG_{45}-*b*-P(4VP-*co*-St) (B).

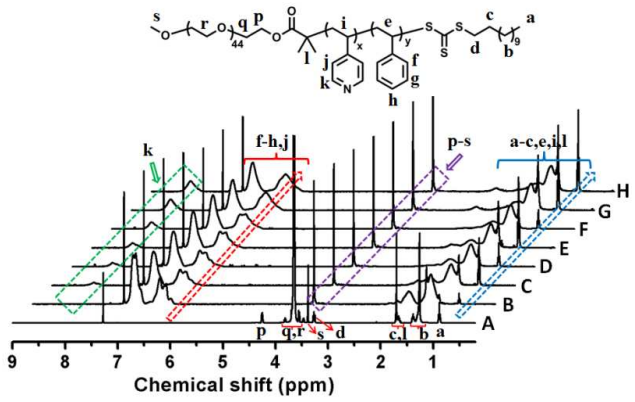

Figure 1. ^{1}H NMR spectra of PEG_{45}-TTC (A), and the synthesized PEG_{45}-*b*-P(4VP-*co*-St) diblock copolymer prepared through the dispersion RAFT copolymerization with the molar ratio of St/4VP at 6/0 (B), 5/1 (C), 4/1 (D), 3/1 (E), 2.5/1 (F), 2/1 (G), 1.5/1 (H). Polymerization conditions: $[St+4VP]_0$:$[PEG_{45}$-$TTC]_0$:$[AIBN]_0$ = 1200:3:1, 70 °C, 24 h (B) and 36 h (C-H).

Figure 1A shows the ^{1}H NMR spectra of the PEG_{45}-TTC macro-RAFT agent. The peaks at δ = 4.25 ppm (*p*) corresponding to the proton of $-CH_2-O(C=O)$ and at δ = 3.64 ppm (*q*, *r*) corresponding to the methylene proton in the poly(ethylene glycol) chains, confirming formation of PEG_{45}-TTC. The esterification efficiency of the hydroxyl-terminated poly(ethylene glycol) can be estimated by the area ratio of the signal at δ = 4.25 ppm (*p*) and the signal at δ = 3.26 ppm (*d*) corresponding to the proton of CH_3-$(CH_2)_{10}$-CH_2S, and it is suggested that more than 96% PEG_{45}-OH is converted into PEG_{45}-TTC. The molecular weight $M_{n,NMR}$ of PEG_{45}-TTC at 2.4 kg/mol can be calculated by comparing the integration areas of the signal at δ = 1.10~1.45 ppm (*b*) and the signal at δ = 3.64 ppm (*q*, *r*). It is found that the molecular weight $M_{n,NMR}$ of PEG_{45}-TTC macro-RAFT agent is very close to the theoretical molecular weight $M_{n,th}$ of the corresponding hydroxyl-terminated poly(ethylene glycol).

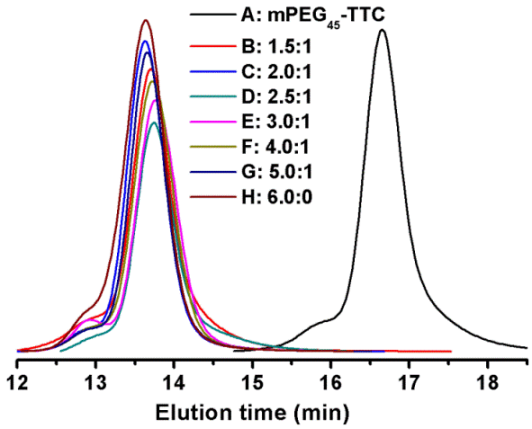

Figure 2. The GPC traces of PEG_{45}-TTC (A), and the synthesized PEG_{45}-*b*-P(4VP-*co*-St) diblock copolymers prepared through the dispersion RAFT copolymerization with the molar ratio of St/4VP at 1.5/1 (B), 2/1 (C), 2.5/1 (D), 3/1 (E), 4/1 (F), 5/1 (G), 6/0 (H). Polymerization conditions: $[St+4VP]_0$:$[PEG_{45}$-$TTC]_0$:$[AIBN]_0$ = 1200:3:1, 70 °C, 36 h (B-G) and 24 h (H).

Figure 2A shows the GPC traces of PEG_{45}-TTC, from which the number-average molecular weight $M_{n,GPC}$ at 2.9 kg/mol and PDI at 1.05 are obtained. The $M_{n,GPC}$ of the PEG_{45}-TTC by GPC analysis is higher than the corresponding $M_{n,NMR}$ by ^{1}H NMR analysis, and the reason is possibly due to the polystyrene standard used in the GPC analysis.

$$M_{n,th} = \frac{[monomer]_0 \times M_{monomer}}{[RAFT]_0} + M_{RAFT} \qquad (1)$$

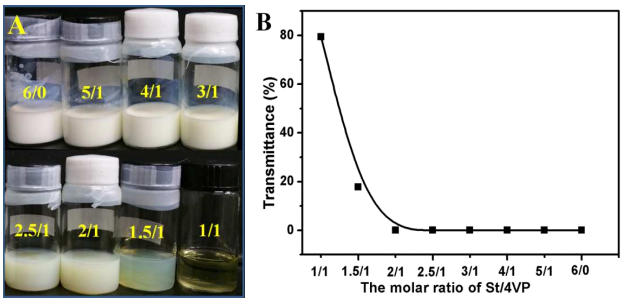

Figure 3. The optical photos (A) and the transmittance of the polymerization solution/dispersion of the PEG_{45}-*b*-P(4VP-*co*-St) diblock copolymer prepared under different St/4VP molar ratio (B).

$$M_{n,NMR} = \frac{4 \times 45 I_{7.9\sim8.6}}{2 I_{3.6}} \times M_{4VP} + \frac{4 \times 45 (I_{6.3\sim7.2} - I_{7.9\sim8.6})}{5 I_{3.6}} \times M_{St} + M_{n,PEG} \qquad (2)$$

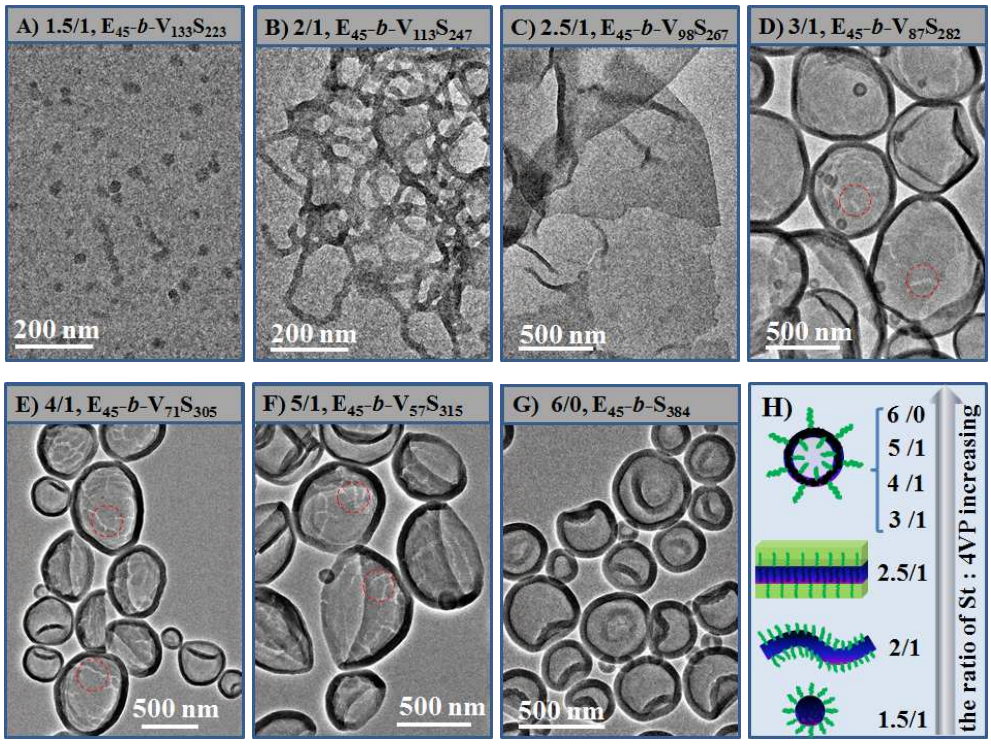

Figure 4. TEM images of the E-*b*-VS diblock copolymer nano-objects prepared through the dispersion RAFT copolymerization with the St/4VP molar ratio at 1.5/1 (A), 2/1 (B), 2.5/1 (C), 3/1 (D), 4/1 (E), 5/1 (F), 6/0 (G), and summary of the nano-objects prepared under different St/4VP molar ratio (H). Polymerization conditions: $[St+4VP]_0:[PEG_{45}\text{-}TTC]_0:[AIBN]_0$ = 1200:3:1, 70 °C, 36 h (A-F) and 24 h (G).

3.2 PEG_{45}-TTC mediated RAFT (co)polymerization

In a general macro-RAFT agent mediated dispersion polymerization, one hydrophobic monomer to form the solvophobic block is added in the polymerization medium and therefore nano-objects of AB diblock copolymer are *in situ* prepared.[35,36,38-45,48-50] In the present study, both the hydrophobic monomer of St and the hydrophilic co-monomer of 4VP are added and therefore nano-objects of the PEG-*b*-P(4VP-*co*-St) diblock copolymer containing a random P(4VP-*co*-St) block are expected to be formed during the PEG-TTC macro-RAFT agent mediated dispersion copolymerization as shown in Scheme 1B. To show the hydrophilic 4VP co-monomer affecting the block copolymer morphology in the dispersion RAFT copolymerization, the subsequent discussion is divided into three sections: (1) the morphology of the PEG-*b*-P(4VP-*co*-St) diblock copolymer nano-objects prepared through the dispersion RAFT copolymerization under different St/4VP monomer ratio is checked, through which the fruitful influence of the 4VP co-monomer on the block copolymer morphology is demonstrated; (2) and the RAFT copolymerization kinetics is explored, and the morphology evolution of the PEG-*b*-P(4VP-*co*-St) diblock copolymer nano-objects during the dispersion RAFT copolymerization is clarified; (3) the morphology comparison between the PEG-*b*-P(4VP-*co*-St) diblock copolymer nano-objects prepared by the dispersion RAFT copolymerization of St/4VP and those of PEG-*b*-PS prepared through the dispersion RAFT polymerization of St is made, in which the morphology difference is demonstrated. In the next discussion, the PEG-*b*-P(4VP-*co*-St) and PEG-*b*-PS diblock copolymers are briefly called E-*b*-VS and E-*b*-S, respectively.

Initially, to check the hydrophilic 4VP co-monomer affecting the block copolymer morphology in the dispersion RAFT copolymerization, the PEG_{45}-TTC macro-RAFT agent mediated dispersion copolymerization of St/4VP in the 80/20 methanol/water mixture under the constant $[St+4VP]_0:[PEG_{45}\text{-}TTC]_0:[AIBN]_0$ = 1200:3:1 but different molar ratio of the feeding St/4VP was performed and then the *in situ* synthesized E-*b*-VS nano-objects were checked. To eliminate the effect of the residual monomers on the morphology of the block copolymer nano-objects, the dispersion RAFT copolymerization of St/4VP was extended to 36 h to ensure high conversion of the St/4VP monomers at 89-94% (Note: the monomer conversion of St/4VP is defined by eq S3). Clearly, this dispersion RAFT copolymerization affords the nano-objects of the E-*b*-VS diblock copolymer with the very similar theoretical molecular weight $M_{n,th}$ based on eq 1.[54]

After the dispersion RAFT copolymerization under different St/4VP molar ratio being quenched, the difference of the E-*b*-VS diblock copolymer nano-objects can be easily judged by naked eyes. As shown in Figure 3A, the PEG_{45}-TTC macro-RAFT agent mediated dispersion polymerization of St affords the milky dispersion of the E-*b*-S diblock nano-objects. With the addition of the hydrophilic 4VP co-monomer, the transmittance of the E-*b*-VS nano-objects increases till a transparent solution is observed at St/4VP = 1/1 (Figure 3B). This is ascribed to the different solubility of the E-*b*-VS diblock copolymer in the polymerization medium of

the 80/20 methanol/water, in which the PEG block is soluble, and the P4VP segment is solvophilic and the PS segment in the P(4VP-*co*-St) block is solvophobic, that is, the higher P4VP content and therefore the better solubility of the E-*b*-VS diblock copolymer. This different appearance of the E-*b*-VS diblock copolymer nano-objects prepared under different St/4VP molar ratio indicates the different block copolymer morphology, which will be discussed subsequently.

The E-*b*-VS nano-objects prepared under different St/4VP molar ratio were collected and the E-*b*-VS diblock copolymer was characterized by ^{1}H NMR analysis and GPC analysis (Figures 1 and 2). As shown in Figure 1, the signal at δ = 7.90~8.60 ppm (*k,* as indicated by the green square corresponding to the proton of pyridine ring next to the *N* atom in the P4VP segment) increases with the feeding 4VP co-monomer, indicating the increasing content of the solvophilic P4VP segments in the E-*b*-VS diblock copolymer. The molecular weight $M_{n,NMR}$ of the diblock copolymer is calculated by comparing the area ratio of the characteristic chemical shift at δ = 3.6 ppm (*p-s*) of the proton in the PEG block to that at δ = 7.90~8.60 ppm (*k*) and at δ = 6.30~7.25 ppm (*f-h, j*) in the P(4VP-*co*-St) block following eq 2, and the results are summarized in Table S1. It is found that the ratio of the PS/P4VP segment in the P(4VP-*co*-St) diblock copolymer is slightly larger than the ratio of the feeding St/4VP, suggesting that the conversion of the St monomer runs slighter faster than that of the 4VP monomer, which will be further discussed subsequently. Based on the GPC analysis, the molecular weight $M_{n,GPC}$ of the E-*b*-S or E-*b*-VS diblock copolymer and its distribution index of PDI are obtained and summarized in Table S1. It is found that the three values of the diblock copolymer molecular weight, $M_{n,NMR}$, $M_{n,th}$, and $M_{n,GPC}$, are close to each other and the molecular weight is narrowly distributed as indicated by the satisfied PDI around at 1.1-1.2, suggesting the good control in the polymer molecular weight during the dispersion RAFT copolymerization. Note: the shoulder in the GPC traces at the high molecular weight side is possibly due to the impurity in the PEG_{45}-TTC macro-RAFT agent; based on the ^{1}H NMR spectra shown in Figure 1A, just 4% of the impurity is immerged in PEG_{45}-TTC, and therefore the impurity exerts very slight influence on the RAFT polymerization; the similar can also found in ref. 55. The characterizations clearly demonstrate that the E-*b*-VS diblock copolymers prepared under $[St+4VP]_0:[PEG_{45}\text{-}TTC]_0:[AIBN]_0$ = 1200:3:1 with different St/4VP molar ratio have similar molecular weight, which affords advantage to check the 4VP-comonomer effect on the morphology of the E-*b*-VS nano-objects.

Figure 4 summarizes the TEM images of the E-*b*-VS diblock copolymer nano-objects synthesized under different St/4VP molar ratio, in which the great influence of the hydrophilic 4VP co-monomer on the morphology of the *in situ* synthesized E-*b*-VS diblock copolymer nano-objects is demonstrated. For example, nanospheres with the average diameter at 27 nm (Figure 4A), lines with the width at 24 nm (Figure 4B), lamellae (Figure 4C), and vesicles with the average size at 200-600 nm (Figure 4D-G) are formed with the St/4VP molar ratio at 1.5/1, 2/1, 2.5/1, 3/1, 4/1, 5/1 and 6/0, respectively, and the evolution of the E-*b*-VS nano-objects with the St/4VP molar ratio is summarized in Figure 4H. Interestingly, slight difference between the E-*b*-VS vesicles (Figure 4D-F) and the E-*b*-S vesicles (Figure 4G) has been found, That is, the membrane of the E-*b*-VS vesicles is cracked as indicated by the red cycles in the TEM images, whereas the E-*b*-S vesicles keep perfect. The reason is not very clearly, and the possible reason is due to the P4VP segment in the P(4VP-*co*-St) block increasing immiscibility of the membrane, which leads to the membrane splitting when the solvent is vaporized during the TEM sampling. It is well documented,[56-58] that the morphology of amphiphilic AB diblock copolymer in the block selective solvent follows the evolution of spheres-to-worms-to-vesicles with the decreasing ratio of the solvophilic A block to the solvophobic B bock. The results mentioned above afford another way to achieve morphology tuning by the changing the ratio of the hydrophilic/hydrophobic segment in a random block through macro-RAFT agent mediated dispersion copolymerization of a binary mixture of hydrophilic/hydrophobic monomers.

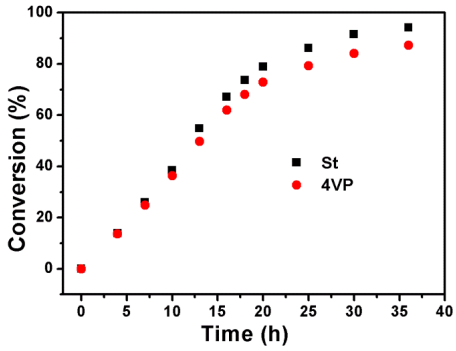

Figure 5. The monomer conversion-time plot for the dispersion RAFT copolymerization of St/4VP. Polymerization conditions: $[St]_0:[4VP]_0:[PEG_{45}\text{-}TTC]_0:[AIBN]_0$ = 900:300:3:1, 70 °C.

3.3 Polymerization kinetics and evolution of the block copolymer morphology during the dispersion RAFT copolymerization

With the encouraging results in hand, the kinetics of the PEG_{45}-TTC macro-RAFT agent mediated dispersion copolymerization typically under $[St]_0:[4VP]_0:[PEG_{45}\text{-}TTC]_0:[AIBN]_0$ = 900:300:3:1 was investigated, and the morphology of the E-*b*-VS diblock copolymer nano-objects with the extension of the P(4VP-*co*-St) block during the dispersion RAFT copolymerization was checked. From the time dependent monomer conversion shown in Figure 5, it found that the conversion of the St monomer runs slighter faster than that of the 4VP co-monomer. Based on polymerization kinetics and the monomer reactivity ratios, $r_{1(St)}$ = 0.11 and $r_{2(4VP)}$ = 0.62, which are approximately calculated by the Alfrey-Price's Q-e equation,[59] it is assumed that the P4VP segment is almost uniformly distributed in the random P(4VP-*co*-St) block. Compared with the PEG_{45}-TTC macro-RAFT agent mediated dispersion polymerization of St under $[St]_0:[PEG_{45}\text{-}TTC]_0:[AIBN]_0$ = 1200:3:1 with other same conditions, the dispersion RAFT copolymerization runs a little slower, and just about 92.4% conversion of the St/4VP monomers is achieved even the polymerization is extended to 36 h (Figure S2). The possible reason is due to the solvophilic P4VP segment in the P(4VP-*co*-St) block, which retards the particle nucleation of the *in situ* synthesized E-*b*-VS diblock copolymer in the polymerization medium of the 80/20 methanol/water mixture.

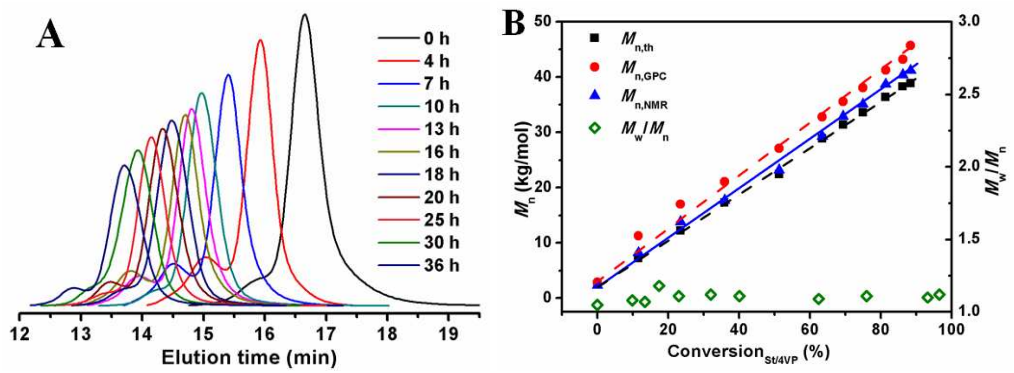

Figure 6. The GPC traces (A) and evolution of the molecular weight and the PDI (M_w/M_n) value (B) of the E-*b*-VS diblock copolymer synthesized through the dispersion RAFT copolymerization of St/4VP. Polymerization conditions can be found in the caption for Figure 5.

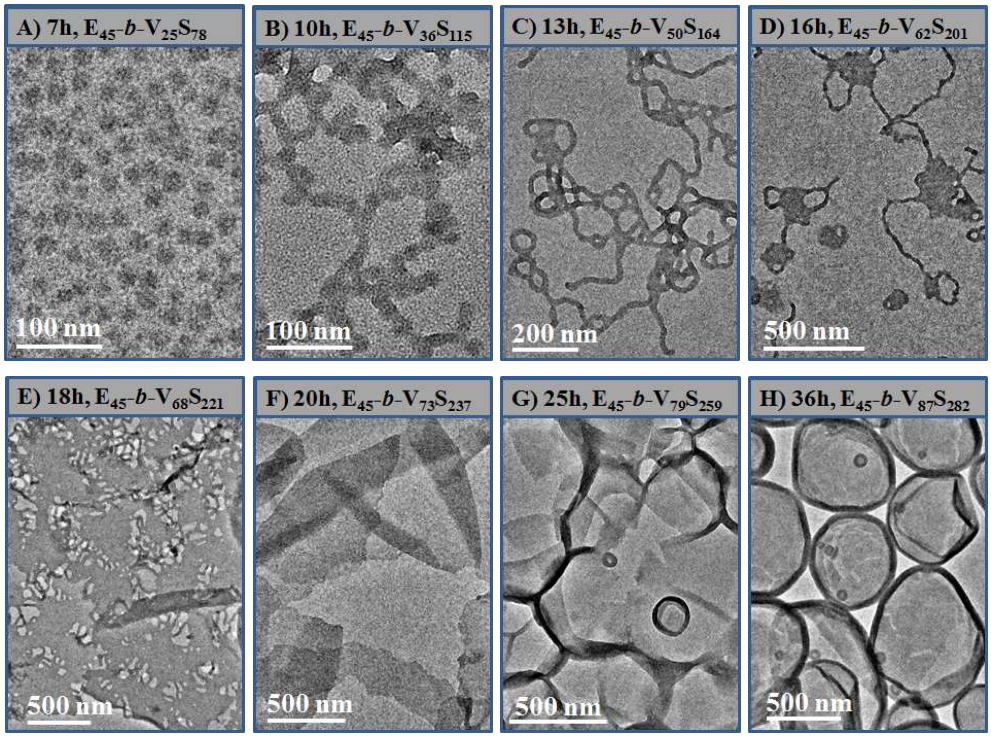

Figure 7. TEM images of the E-*b*-VS diblock copolymer nano-objects prepared at different polymerization times. Polymerization conditions can be found in the caption for Figure 5.

Figures 6A shows the GPC traces of the E-*b*-VS diblock copolymers synthesized at different polymerization times. Based on the GPC analysis, the molecular weight $M_{n,GPC}$ and PDI of the diblock copolymers around at 1.1-1.2 are obtained, and the results are summarized in Figure 6B and Table S1. As shown in Figure 6B, the molecular weight $M_{n,GPC}$ of the E-*b*-VS diblock copolymers increases linearly with the conversion of the St/4VP monomers, which is as similar as those in the PEG_{45}-TTC macro-RAFT agent mediated dispersion polymerization of St (Figure S3). These E-*b*-VS diblock copolymers are also characterized by ^{1}H NMR analysis. From the ^{1}H NMR spectra typically shown in Figure 1, the molecular weight of the E-*b*-VS diblock copolymers is calculated by eq 2. It is found that $M_{n,GPC}$ by GPC analysis, $M_{n,NMR}$ by ^{1}H NMR analysis, and the theoretical $M_{n,th}$ of the E-*b*-VS diblock copolymers are close to each other. These results confirm the well-controlled RAFT dispersion copolymerization.

Figure 7 summarizes the TEM images of the E-*b*-VS diblock copolymer nano-objects synthesized through the PEG_{45}-TTC macro-RAFT agent mediated dispersion polymerization at different polymerization times. Note: to clearly evaluate the DP of the newly formed P(4VP-*co*-St) block affecting the block copolymer morphology, the detail composition of the E-*b*-VS diblock copolymers at different polymerization times is indicated out as insets in the TEM images. As indicated by the TEM images, the morphology of the E-*b*-VS diblock copolymer nano-objects undergoes the evolution from nanospheres (Figure 7A) to lines

(Figures 7B and C), to lamellae (Figure 7F), and finally to vesicles (Figure 7H) with the extension of the P(4VP-*co*-St) block. Besides, the intermediate morphologies of the E-*b*-VS diblock copolymer such as the line-lamellae joint (Figures 7D and E) and the immature vesicles (Figure 7G) are observed. Whereas, in the PEG_{45}-TTC macro-RAFT agent mediated dispersion polymerization of St, the E-*b*-S vesicles are just observed (Figure S4). This suggests that the macro-RAFT agent mediated dispersion copolymerization of a binary mixture of hydrophilic/hydrophobic monomers may be a valid method of the *in situ* synthesis of block copolymer nano-objects with abundant morphologies.

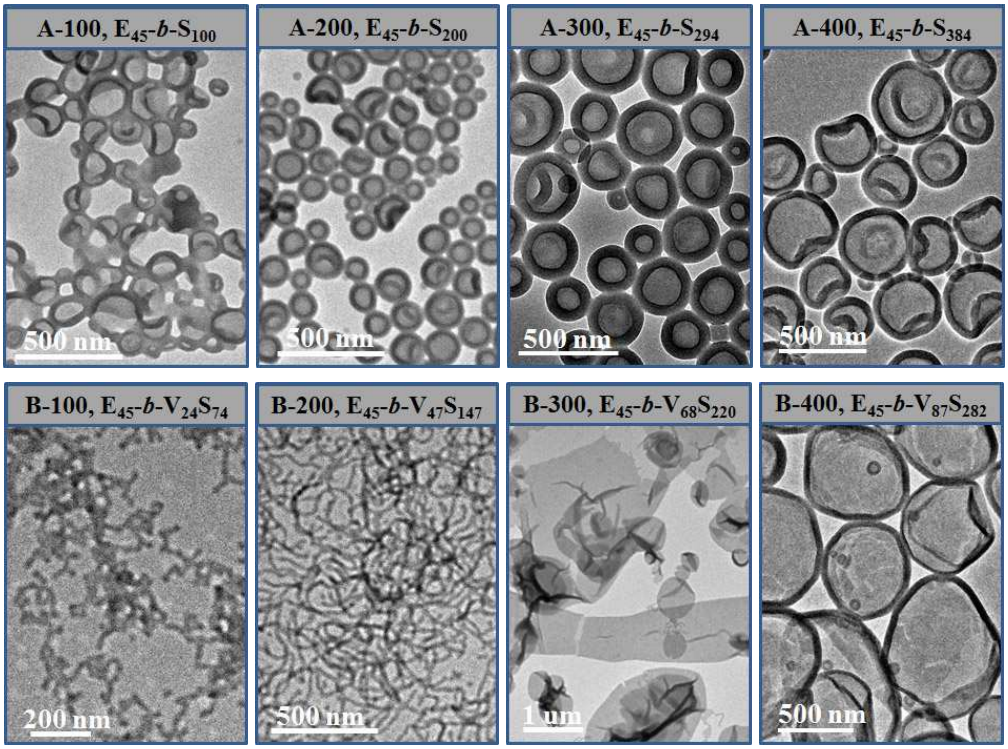

Figure 8. TEM images of the diblock copolymer nano-objects of E-*b*-S (A) and E-*b*-VS (B) through the dispersion RAFT (co)polymerization under $[St]_0$:$[PEG_{45}$-$TTC]_0$:$[AIBN]_0$ = 300~1200:300:3:1 70 ^{0}C for 24 h (A-100~400) or $[St+4VP]_0$:$[PEG_{45}$-$TTC]_0$:$[AIBN]_0$ = 300~1200:300:3:1 at 70 ^{0}C for 36 h (B-100~400).

3.4 Comparison between the morphology of E-*b*-VS and E-*b*-S

It has been demonstrated that the morphology of amphiphilic block copolymer is firmly dependent on the solvophobic/solvophilic ratio.[35,37-44,49,50,56-58] As discussed above, the present macro-RAFT agent mediated dispersion RAFT copolymerization affords the nano-objects of the E-*b*-VS diblock copolymer containing a random P(4VP-*co*-St) block. Since the P(4VP-*co*-St) block contains both a hydrophilic and a hydrophobic segment, the solubility character and therefore the morphology of the E-*b*-VS nano-objects can be easily tuned just by changing the P(4VP-*co*-St) block. In the above discussion (Figure 4), it is shown that the morphology of the E-*b*-VS diblock copolymer nano-objects with the similar chain length (or DP) of the P(4VP-*co*-St) block can be tuned by the ratio of the PS/P4VP segments in the P(4VP-*co*-St) block. In this section, the morphology of the E-*b*-VS diblock copolymer nano-objects with the similar ratio of the PS/P4VP segments in the P(4VP-*co*-St) block but the different chain length of the P(4VP-*co*-St) block is checked and compared with those of the E-*b*-S diblock copolymer nano-objects. To prepare these block copolymer nano-objects, the dispersion RAFT copolymerization under $[St+4VP]_0$:$[PEG_{45}$-$TTC]_0$:$[AIBN]_0$ = 300~1200:300:3:1 with the constant molar ratio of St/4VP at 3/1 was performed, and the morphology of the E-*b*-VS block copolymer nano-objects was checked. Besides, to eliminate the effect of the residual monomers on the morphology of the block copolymer nano-objects, the dispersion RAFT copolymerization was extended to 36 h to ensure the high monomer conversion similarly around 92-100%.

As shown in Figure 8A, vesicles of E-*b*-S are formed during the dispersion RAFT polymerization at four DP cases of 100 (Figure 8A-100), 200 (Figure 8A-200), 294 (Figure 8A-300) and 384 (Figure 8A-400). Note: in the Figure label of A-XX or B-XX, the value of XX represents the target DP of the PS block or the P(4VP-*co*-St) block at 100% monomer conversion, and the DP for the P(4VP-*co*-St) block is defined by the sum of the repeat units of the PS and P4VP segment in the P(4VP-*co*-St) block. Whereas, when the hydrophilic co-monomer of 4VP is added with molar ratio of St/4VP at 3/1, four different E-*b*-VS nano-objects including rods (Figure 8B-100), lines (Figure 8B-200), lamellae (Figure 8B-300) and vesicles (Figure 8B-400) are formed at the four DP cases. The results clearly show that the morphology of the E-*b*-VS diblock copolymer prepared through the dispersion RAFT copolymerization is much different from that of the E-*b*-S diblock copolymer even at the same/similar DP of the PS or P(4VP-*co*-St) block. The reason is of course due to the different solvophobic/solvophilic ratio in the two diblock copolymers of E-*b*-S and E-*b*-VS. Besides, the different morphology

of the two diblock copolymer also arises from the different nucleation of the two diblock copolymers, since it is observed that the nucleation of E-*b*-S occurs earlier that of E-*b*-VS under the other similar condition during the dispersion RAFT polymerization. Nevertheless, the results suggest that the dispersion RAFT copolymerization of the mixture of the hydrophilic/hydrophobic monomers possibly has the advantage in tuning the block copolymer morphology over the dispersion RAFT polymerization of a single hydrophobic monomer.

4 Conclusions

The macro-RAFT agent mediated dispersion polymerization is a valid method to prepared block copolymer nano-objects. In this study, to further conveniently tune the block copolymer morphology, the macro-RAFT agent mediated dispersion copolymerization of two monomers, in which one is hydrophobic and the other is hydrophilic, is proposed. The PEG-TTC macro-RAFT agent mediated dispersion copolymerization of St/4VP affords the *in situ* synthesis of the nano-objects of the PEG-*b*-P(4VP-*co*-St) diblock copolymer containing a P(4VP-*co*-St) block. It is found that, the morphology of the PEG-*b*-P(4VP-*co*-St) diblock copolymer nano-objects can be easily tuned either by the DP of the random P(4VP-*co*-St) block or the molar ratio of the PS/P4VP segments in the random P(4VP-*co*-St) block. That is, with the DP of the P(4VP-*co*-St) block increasing, the morphology of the PEG-*b*-P(4VP-*co*-St) nano-objects undergoes the evolution from nanospheres to lines, further to lamellae and finally to vesicles; and with the increasing molar ratio of PS/P4VP segments in the random P(4VP-*co*-St) block, the morphology of the PEG-*b*-P(4VP-*co*-St) nano-objects changes form vesicles to nanospheres. The PEG-TTC macro-RAFT agent mediated dispersion copolymerization of St/4VP is compared with the PEG-TTC macro-RAFT agent mediated dispersion polymerization of St, and the advantage of the dispersion RAFT copolymerization in tuning the block copolymer morphology is demonstrated. The dispersion RAFT copolymerization affords great convenience to tune block copolymer morphology under dispersion conditions, and it is believed to a promising extension of the polymerization-induced self-assembly (PISA) under dispersion RAFT polymerization.

Acknowledgements

The financial support by National Science Foundation of China (№ 21274066 and 21474054) and PCSIRT (IRT1257) is gratefully acknowledged.

Notes and references

1 G. Riess, *Prog. Polym. Sci.*, 2003, **28**, 1107-1170.
2 M. J. Monteiro and M. F. Cunningham, *Macromolecules*, 2012, **45**, 4939-4957.
3 J.-T. Sun, C.-Y. Hong and C.-Y. Pan, *Polym. Chem.*, 2013, **4**, 873-881.
4 Y. Mai and A. Eisenberg, *Chem. Soc. Rev.*, 2012, **41**, 5969-5985.
5 H. Cui, Z. Chen, S. Zhong, K. L. Wooley and D. J. Pochan, *Science*, 2007, **317**, 647-650.
6 N. P. Truong, J. F. Quinn, M. V. Dussert, N. B. T. Sousa, M. R. Whittaker and T. P. Davis, *ACS Macro Lett.*, 2015, **4**, 381-386.
7 L. Yin and M. A. Hillmyer, *Macromolecules*, 2011, **44**, 3021-3028.
8 R. Fenyves, M. Schmutz, I. J. Horner, F. V. Bright and J. Rzayev, *J. Am. Chem. Soc.*, 2014, **136**, 7762-7770.
9 M. J. Barthel, U. Mansfeld, S. Hoeppener, J. A. Czaplewska, F. H. Schacher and U. S. Schubert, *Soft Matter*, 2013, **9**, 3509-3520.
10 B. Ni, M. Huang, Z. Chen, Y. Chen, C.-H. Hsu, Y. Li, D. Pochan, W.-B. Zhang, S. Z. D. Cheng and X.-H. Dong, *J. Am. Chem. Soc.* 2015, **137**, 1392-1395.
11 C. Herfurth, P. M. de Molina, C. Wieland, S. Rogers, M. Gradzielski and A. Laschewsky, *Polym. Chem.*, 2012, **3**, 1606-1617.
12 W. Kim, J. Thévenot, E. Ibarboure, S. Lecommandoux and E. L. Chaikof, *Angew. Chem. Int. Ed.*, 2010, **49**, 4257-4260.
13 R. T. Pearson, N. J. Warren, A. L. Lewis, S. P. Armes and G. Battaglia, *Macromolecules*, 2013, **46**, 1400-1407.
14 J. Xu, K. Wang, J. Li, H. Zhou, X. Xie and J. Zhu, *Macromolecules*, 2015, **48**, 2628-2636.
15 J. B. Gilroy, D. J. Lunn, S. K. Patra, G. R. Whittell, M. A. Winnik and I. Manners, *Macromolecules*, 2012, **45**, 5806-5815.
16 O. Colombani, M. Ruppel, M. Burkhardt, M. Drechsler, M. Schumacher, M. Gradzielski, R. Schweins and A. H. E. Müller, *Macromolecules*, 2007, 40, 4351-4362.
17 C. Pietsch, U. Mansfeld, C. Guerrero-Sanchez, S. Hoeppener, A. Vollrath, M. Wagner, R. Hoogenboom, S. Saubern, S. H. Thang, C. R. Becer, J. Chiefari and U. S. Schubert, *Macromolecules*, 2012, **45**, 9292-9302.
18 Y. He, Z. Li, P. Simone and T. P. Lodge, *J. Am. Chem. Soc.*, 2006, **128**, 2745-2750.
19 T. Rudolph, A. Nunns, A. M. Schwenkea and F. H. Schacher, *Polym. Chem.*, 2015, **6**, 1604-1612.
20 V. A. Vasantha, S. Jana, S. S.-C. Lee, C.-S. Lim, S. L.-M. Teo, A. Parthiban and J. G. Vancsoa, *Polym. Chem.*, 2015, **6**, 599-606.
21 J. Dupont, G. Liu, K. Niihara, R. Kimoto and H. Jinnai, *Angew. Chem. Int. Ed.*, 2009, **48**, 6144-6147.
22 Z. Ge and S. Liu, *Macromol. Rapid Commun.*, 2009, **30**, 1523-1532.
23 M. T. Savoji, S. Strandman and X. X. Zhu, *Langmuir*, 2013, 29, 6823-6832.
24 W. Wang, H. Liu, M. Mu, H. Yin and Y. Feng, *Polym. Chem.*, 2015, 6, 2900-2908.
25 D. B. Wright, J. P. Patterson., A. Pitto-Barry, P. Cotanda, C. Chassenieux, O. Colombani and R. K. O′Reilly, *Polym. Chem.*, 2015, 6, 2761-2768.
26 E. Karjalainen, N. Chenna, P. Laurinmäki, S. J. Butcher and H. Tenhu, *Polym. Chem.*, 2013, 4, 1014-1024.
27 B. Charleux, G. Delaittre, J. Rieger and F. D'Agosto, *Macromolecules*, 2012, **45**, 6753-6765.
28 S. Binauld, L. Delafresnaye, B. Charleux, F. D'Agosto, and M. Lansalot, *Macromolecules*, 2014, **47**, 3461-3472.

29 N. P. Truong, M. V. Dussert, M. R. Whittaker, J. F. Quinn and T. P. Davis, *Polym. Chem.*, 2015, **6**, 3865-3874.
30 Z. Jia, V. A. Bobrin, N. P. Truong, M. Gillard and M. J. Monteiro, *J. Am. Chem. Soc.*, 2014, **136**, 5824-5827.
31 R. W. Simms, T. P. Davis and M. F. Cunningham, *Macromol. Rapid Commun.*, 2005, **26**, 592-596.
32 D. E. Ganeva, E. Sprong, H. de Bruyn, G. G. Warr, C. H. Such and B. S. Hawkett, *Macromolecules*, 2007, **40**, 6181-6189.
33 G. Liu, Q. Qiu and Z. An, *Polym. Chem.*, 2012, **3**, 504-513.
34 C. A. Figg, A. Simula, K. A. Gebre, B. Tucker, D. M. Haddleton and Brent S. Sumerlin, *Chem. Sci.*, 2015, 6, 1230-1236.
35 W. Zhao, G. Gody, S. Dong, P. B. Zetterlund and S. Perrier, *Polym. Chem.*, 2014, 5, 6990-7003.
36 Y. Pei, L. Thurairajah, O. R. Sugita and A. B. Lowe, *Macromolecules*, 2015, **48**, 236-244.
37 Y. Pei and A. B. Lowe, *Polym. Chem.*, 2014, **5**, 2342-2351.
38 W.-J. Zhang, C.-Y. Hong and C.-Y. Pan, *Macromolecules*, 2014, **47**, 1664-1671.
39 W.-D. He, X.-L. Sun, W.-M. Wan and C.-Y. Pan, *Macromolecules*, 2011, **44**, 3358-3365.
40 L. A. Fielding, M. J. Derry, V. Ladmiral, J. Rosselgong, A. M. Rodrigues, L. P. D. Ratcliffe, S. Sugihara and S. P. Armes, *Chem. Sci.*, 2013, **4**, 2081-2087.
41 M. J. Derry, L. A. Fielding and S. P. Armes, *Polym. Chem.*, 2015, **6**, 3054-3062.
42 A. Blanazs, J. Madsen, G. Battaglia, A. J. Ryan and S. P. Armes, *J. Am. Chem. Soc.*, 2011, **133**, 16581-16587.
43 M. Semsarilar, V. Ladmiral, A. Blanazs and S. P. Armes, *Polym. Chem.*, 2014, **5**, 3466-3475.
44 S. Sugihara, A. Blanazs, S. P. Armes, A. J. Ryan and A. L. Lewis, *J. Am. Chem. Soc.*, 2011, **133**, 15707-15713.
45 N. J. Warren, O. O. Mykhaylyk, A. J. Ryan, M. Williams, T. Doussineau, P. Dugourd, R. Antoine, G. Portale and S. P. Armes, *J. Am. Chem. Soc.*, 2015, **137**, 1929-1937.
46 Q. Li, C. Gao, S. Li, F. Huo and W. Zhang, *Polym. Chem.*, 2014, **5**, 2961-2972.
47 P. Shi, Q. Li, X. He, S. Li, P. Sun and W. Zhang, *Macromolecules*, 2014, **47**, 7442-7452.
48 Y. Su, X. Xiao, S. Li, M. Dan, X. Wang and W. Zhang, *Polym. Chem.*, 2014, **5**, 578-587.
49 X. Xiao, S. He, M. Dan, Y. Su, F. Huo and W. Zhang, *J. Polym. Sci., Part A: Polym. Chem.*, 2013, **51**, 3177-3190.
50 M. Dan, F. Huo, X. Zhang, X. Wang and W. Zhang, *J. Polym. Sci., Part A: Polym. Chem.*, 2013, **51**, 1573-1584.
51 J. T. Lai, D. Filla and R. Shea, *Macromolecules*, 2002, **35**, 6754-6756.
52 Y. He and T. P. Lodge, *Macromolecules*, 2008, **41**, 167-174.
53 C. Gao, S. Li, Q. Li, P. Shi, S. A. Shah and W. Zhang, *Polym. Chem.*, 2014, *5*, 6957-6966.
54 H. De Brouwer, M. A. J. Schellekens, B. Klumperman, M. J. Monteiro and A. L. German, *J. Polym. Sci., Part A: Polym. Chem*., 2000, **38**, 3596.
55 N. J. Warren, O. O. Mykhaylyk, D. Mahmood, A. J. Ryan and S. P. Armes, *J. Am. Chem. Soc.*, 2014, **136**, 1023-1033.
56 L. A. Fielding, J. A. Lane, M. J. Derry, O. O. Mykhaylyk and S. P. Armes, *J. Am. Chem. Soc.*, 2014, **136**, 5790-5798.
57 L. Zhang and A. Eisenberg, *J. Am. Chem. Soc.*, 1996, **118**, 3168-3181.
58 S. Kessel, N. P. Truong, Z. Jia and M. J. Monteiro, *J Polym Sci Part A: Polym Chem.*, 2012, **50**, 4879-4887.
59 T. Alfrey and C. C. Price, J. *Polym. Sci.* 1947, **2**, 101-106.

For Table of Contents use only

Macro-RAFT agent mediated dispersion copolymerization: a small amount of solvophilic co-monomer leads to a great change

Pengfei Shi, Heng Zhou, Chengqiang Gao, Shuang Wang, Pingchuan Sun* and Wangqing Zhang*

Key Laboratory of Functional Polymer Materials of the Ministry of Education, Collaborative Innovation Center of Chemical Science and Engineering (Tianjin), Institute of Polymer Chemistry, Nankai University, Tianjin 300071, China.

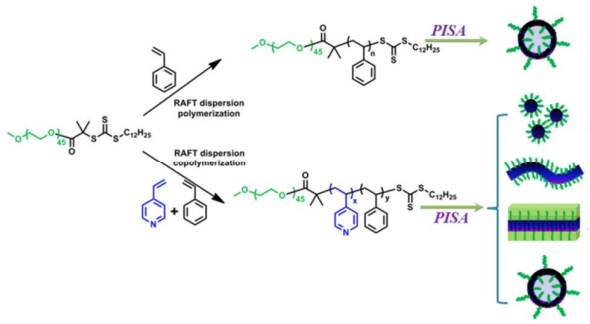

The macro-RAFT agent mediated dispersion copolymerization of two monomers is performed, and the block copolymer morphology can be easily tuned.